Journal of Cerebral Blood Flow and Metabolism
13:656–667 © 1993 The International Society of Cerebral Blood Flow and Metabolism
Published by Raven Press, Ltd., New York

Measurement of Benzodiazepine Receptor Number and Affinity in Humans Using Tracer Kinetic Modeling, Positron Emission Tomography, and [^{11}C]Flumazenil

Julie C. Price, Helen S. Mayberg, Robert F. Dannals, Alan A. Wilson, Hayden T. Ravert, Bernard Sadzot, Zachary Rattner, *Allyn Kimball, †Marc A. Feldman, and J. James Frost

*Division of Nuclear Medicine, Department of Radiology, Division of Radiation Health Sciences, Department of Environmental Health Sciences, *Department of Biostatistics, and †Department of Anesthesiology, Johns Hopkins Medical Institutions, Baltimore, Maryland, U.S.A.*

Summary: Kinetic methods were used to obtain regional estimates of benzodiazepine receptor concentration (B_{max}) and equilibrium dissociation constant (K_d) from high and low specific activity (SA) [^{11}C]flumazenil ([^{11}C] Ro 15-1788) positron emission tomography studies of five normal volunteers. The high and low SA data were simultaneously fit to linear and nonlinear three-compartment models, respectively. An additional inhibition study (pretreatment with 0.15 mg/kg of flumazenil) was performed on one of the volunteers, which resulted in an average gray matter K_1/k_2 estimate of 0.68 ± 0.08 ml/ml (linear three-compartment model, nine brain regions). The free fraction of flumazenil in plasma (f_1) was determined for each study (high SA f_1: 0.50 ± 0.03; low SA f_1: 0.48 ± 0.05). The free fraction in brain (f_2) was calculated using the inhibition K_1/k_2 ratio and each volunteer's mean f_1 value (f_2 across volunteers = 0.72 ± 0.03 ml/ml). Three methods (Methods I–III) were examined. Method I determined five kinetic parameters simultaneously [K_1, k_2, k_3 ($=k_{on}f_2B_{max}$), k_4, and $k_{on}f_2$/SA] with no a priori constraints. An average k_{on} value of 0.030 ± 0.003 nM^{-1} min^{-1} was estimated for receptor-rich regions using Method I. In Methods II and III, the $k_{on}f_2$/SA parameter was specifically constrained using the Method I value of k_{on} and the volunteer's values of f_2 and low SA (Ci/μmol). Four parameters were determined simultaneously using Method II. In Method III, K_1/k_2 was fixed to the inhibition value and only three parameters were estimated. Method I provided the most variable results and convergence problems for regions with low receptor binding. Method II provided results that were less variable but very similar to the Method I results, without convergence problems. However, the K_1/k_2 ratios obtained by Method II ranged from 1.07 in the occipital cortex to 0.61 in the thalamus. Fixing the K_1/k_2 ratio in Method III provided a method that was physiologically consistent with the fixed value of f_2 and resulted in parameters with considerably lower variability. The average B_{max} values obtained using Method III were 100 ± 25 nM in the occipital cortex, 64 ± 18 nM in the cerebellum, and 38 ± 5.5 nM in the thalamus; the average K_d was 8.9 ± 1.0 nM (five brain regions). **Key Words:** Benzodiazepine receptors—[^{11}C]Flumazenil—Human brain—Kinetic modeling—Positron emission tomography.

Efforts to image central benzodiazepine (BZ) receptors using positron emission tomography (PET) began with the agonist [^{11}C]flunitrazepam (Comar et al., 1979, 1981). Subsequently, the antagonist [^{11}C]flumazenil ([^{11}C]Ro 15-1788) Mazière et al., 1983; Hantraye et al., 1984, 1988; Persson et al., 1985; Samson et al., 1985; Shinotoh et al., 1986) and the cyclopyrrolone [^{11}C]suriclone (Frost et al., 1986) were used. Of these ligands, [^{11}C]flumazenil is superior for the PET imaging of BZ receptors due to its kinetic and pharmacological attributes and has been widely used for human studies.

PET studies of [^{11}C]flumazenil binding have demonstrated a rapid uptake and a high specific/

Received January 8, 1992; final revision received January 13, 1993; accepted February 10, 1993.

Address correspondence and reprint requests to Dr. J. J. Frost at Department of Radiology, Johns Hopkins University School of Medicine, Rm. B1-130, 600 N. Wolfe St., Baltimore, MD 21205, U.S.A.

Abbreviations used: BZ, benzodiazepine; CT, computed tomography; CV, coefficient of variation; PET, positron emission tomography; SA, specific activity.

nonspecific ratio in human brain (Samson et al., 1985; Shinotoh et al., 1986). The main metabolite of [^{11}C]flumazenil has been shown to have a negligible contribution to the PET brain signal (Persson et al., 1989*a*) as a result of brain uptake. Flumazenil can be administered in large doses (Darragh et al., 1983), allowing PET studies at several specific activities (SAs) to be performed. These characteristics are advantageous for the quantification of BZ receptor binding parameters in vivo.

The quantification of [^{11}C]flumazenil PET studies has included the measurement of receptor occupancy after the administration of clonazepam (Shinotoh et al., 1989) and Cl 218,872 (de la Sayette et al., 1991). A linear two-compartment model has been used to quantify the kinetics of high SA [^{11}C]flumazenil and regional transport rates, and ligand distribution volumes have been estimated (Koeppe et al., 1991). The distribution volumes reflect specific binding withstanding changes in ligand delivery (Holthoff et al., 1991).

However, the majority of the quantitative effort has been aimed at estimating BZ receptor concentration (B_{max}) and equilibrium dissociation constant (K_d) in vivo. Estimates of B_{max} and K_d have been obtained for a variety of brain regions using pseudoequilibrium data acquired from multiple (Pappata et al., 1988; Persson et al., 1989*b*; Iyo et al., 1991) and dual (Savic et al., 1988; Blomqvist et al., 1990; Abadie et al., 1992) SA [^{11}C]flumazenil PET studies. Pseudoequilibrium is assumed to exist when the ratio of the estimated free and bound ligand concentrations is constant over time and when changes in the bound concentration become small. In addition, Blomqvist et al. (1990) estimated neocortical BZ receptor binding parameters using kinetic modeling.

In the above-referenced studies, the ligand was administered by bolus injection, which does not allow true equilibrium to be established during the time frame of the PET study. The majority of these studies used reference region data as the free ligand concentration. Therefore, these approaches relied on one or both of the following assumptions: (a) The pseudoequilibrium data accurately represented the true equilibrium data, and (b) nonspecific binding was negligible.

The primary goal of this work was to use kinetic methods to obtain regional estimates of human BZ receptor B_{max} and K_d from high and low SA [^{11}C]flumazenil PET data acquired after bolus injection of ligand. Linear and nonlinear three-compartment models were simultaneously fit to the regional data with and without the use of reference region data while accounting for nonspecific binding.

METHODS

Chemistry

HPLC purifications and analyses were performed on a previously described system (Dannals et al., 1986). The HPLC columns used were either (A) Alltech Econosil C18 (250 mm × 10 mm) or (B) Alltech Econosil C18 (250 mm × 4.6 mm). Peak areas were measured using Hewlett-Packard 3390A recording integrators. Isolated radiochemical yields were determined with a Capintec CRC-5R dose calibrator.

[^{11}C]Iodomethane was prepared as described previously (Dannals et al., 1990) and trapped in a solution of Ro 15-5528 (1 mg) in dimethyl-formamide (DMF) (200 μl) at −70°C. Tetrabutylammonium hydroxide (10 μl of a 0.4 *M* aqueous solution) was added and the reaction mixture was heated to 80°C for 2 min. The mixture was diluted with 200 μl of mobile phase and the entire solution was transferred to an HPLC injector loop. Purification by HPLC was accomplished using column A eluted with a mobile phase of acetonitrile/water (0.1 *M* ammonium formate) (25:75) at a flow of 11 ml/min ($k'_{Ro\ 15\text{-}1788}$ = 6.6, $k'_{Ro\ 15\text{-}5528}$ = 3.3). The radioactive peak corresponding to the desired product was collected in a rotary evaporator and the solvent was evaporated to dryness under reduced pressure. The residue was dissolved in sterile, normal saline (7 ml) and filtered through a sterile 0.22-μm filter (Gelman Acrodisc) into a sterile, pyrogen-free evacuated vial containing sterile sodium bicarbonate solution (3 ml, 8.4%). The pH of the final solution was ~7.5. Chemical and radiochemical purity and the specific activity of the formulated product were assayed by analytical HPLC (Dannals et al., 1990) using column B eluted with a mobile phase of acetonitrile/water (0.1 *M* ammonium formate) (30:70) at a flow rate of 4 ml/min ($k'_{Ro\ 15\text{-}1788}$ = 3.3, $k'_{Ro\ 15\text{-}5528}$ = 2.1).

Radiochemical yields of 20–30% (uncorrected) from [^{11}C]iodomethane were obtained 17–19 min from the end of bombardment. Radiochemical purity was >99% and SAs of 1,500–3,600 Ci/mmol were obtained at the end of synthesis.

PET imaging

Five healthy men between the ages of 20 and 43 years were recruited by advertisement and gave informed consent to participate in the PET study. None of the volunteers had a past history of psychiatric illness, neurological disease, or drug abuse. None was taking BZs at the time of the studies.

Each volunteer was fitted with a thermoplastic mask that was used in conjunction with x-ray computed tomography (CT) to localize the planes of interest for the PET study, as previously described (Frost et al., 1989; Sadzot et al., 1991, 1992). The imaging planes were parallel to the glabellar-inion line. The most caudal plane included the inferior temporal cortex and the cerebellum, while the thalamus and midtemporal and occipital cortices were included in the middle plane. The three image planes were simultaneously acquired 32 mm apart using a Neuro-ECAT PET scanner, as previously described (Hoffman et al., 1983). The PET data were acquired over 14 time intervals of varying length with midpoints of 1.5, 3.5, 5.5, 10, 13, 16, 22, 28, 34, 40, 46, 56, 67, and 84 min for a total scan time of 90 min. The images were decay and attenuation corrected (calculated method). Region-of-interest templates were created for each plane using the summed

PET image (from 10 to 30 min postinjection) and CT scan of that plane.

Each volunteer participated in paired high and low SA [^{11}C]flumazenil PET studies conducted ~2.5 h apart on the same day. One volunteer also participated in a third PET study, which involved the administration of high SA [^{11}C]flumazenil after pretreatment with 0.15 mg/kg of unlabeled flumazenil (inhibition study). Approximately 20 mCi of [^{11}C]flumazenil was administered by bolus injection for each study. The mean high SA was 2,346 ± 777 Ci/mmol and the mean low SA was 12.4 ± 3.6 Ci/mmol.

Plasma and blood analyses

Plasma radioactivity concentrations were obtained from arterial blood samples and used in the determination of the time course of radioactivity, the kinetics of drug metabolism, and the free fraction of flumazenil.

Time course of total radioactivity. Approximately 20 arterial blood samples were obtained during the initial 2 min of the study and 20 more samples were collected over the remainder of the 90-min time frame of the study, as described previously (Frost et al., 1989; Sadzot et al., 1991, 1992). Samples were placed in heparinized tubes and centrifuged, and the radioactivity concentrations of the plasma aliquots were determined.

Flumazenil metabolism. Arterial blood samples were acquired prior to injection and at 5, 10, 15, 45, and 90 min postinjection for the determination of radiolabeled metabolites in plasma. A two-part separation process was used in this determination. The first step involved sequentially passing the plasma sample, 5 ml of H_2O buffered with 0.1 N ammonium formate, and 2 ml of methanol through a C-18 reverse-phase Sep-Pak (Waters Associates). In the second step, the radioactivity in the methanol eluant was diluted with 0.1 N ammonium formate to a concentration ratio of 50% methanol/50% buffer, applied to a C-18 reverse-phase analytical HPLC column (Waters Associates), and eluted with a mobile phase of the same concentration ratio at a flow rate of 2 ml/min.

The extraction efficiency was evaluated at each step of the Sep-Pak separation to calculate an overall final extraction. The preinjection blood sample, with [^{11}C]flumazenil added, was used as a control to determine whether metabolites were produced in vitro and the extraction efficiency of the parent drug. Descriptions of the general procedure are available in earlier publications (Frost et al., 1989; Sadzot et al., 1991, 1992).

Free fraction of flumazenil. Prior to injection, ~5 ml of arterial blood was collected and used to evaluate the free fraction of flumazenil in plasma (f_1). [^{11}C]Flumazenil (~10 μCi) was added to a 1-ml plasma sample and to a 1-ml sample of 50 m*M* Tris buffer (pH 7.4 at room temperature). Aliquots (0.4 ml) of these standard samples were pipetted into Centrifree micropartition systems (Amicon) and centrifuged for 20 min at 1,500 rpm in a fixed angle (35°) rotor centrifuge. The ratio of counts in the plasma ultrafiltrate to that in the plasma standard (X) and the similar ratio for the buffer (Y) were used to calculate f_1, where $f_1 = (X/Y) * \omega$ [ω = 0.94 ml water/ml plasma (Altman, 1961)]. Previous publications of neuroreceptor binding studies have also included methods for the determination of the plasma free fraction (Perlmutter et al., 1989; Sawada et al., 1990; Sadzot et al., 1991, 1992).

An additional experiment was performed to determine the adsorption of the standard samples to the plastic test tubes used in the experiments. This was examined by preparing several 1-ml plasma and buffer standard samples that were allowed to sit for 15, 25, 35, 45, and 55 min. At each of these times, the radioactivity concentrations of the standard samples were determined (total). The test tube was then emptied, washed with distilled water, and assayed for radioactivity (empty). Percentages of (empty/total) * 100 were calculated.

Blood analyses. Blood chemistry and toxicology (alcohol, acetone, and acetaldehyde) screens were performed on whole-blood samples that were obtained from the volunteers prior to the first injection.

The partitioning of radioactivity between the red blood cells and plasma was examined for the last two volunteers. These determinations were performed on arterial blood samples collected for each study at 5, 10, 15, 45, and 90 min postinjection.

Kinetic methods

The PET data were analyzed using a conventional three-compartment model (Fig. 1). The intravascular space contains the unmetabolized drug in plasma (C_1) and the two extravascular brain spaces contain the free and nonspecifically bound drug (C_2) and the drug specifically bound to the receptor of interest (C_3).

It was assumed that only the concentrations in the brain compartments gave rise to the observed PET signal and that any contribution from the intravascular space was negligible. Therefore, the calculated model solution (C_{MOD}) was the sum of the concentrations in the two brain compartments:

$$C_{MOD}(t) = C_2(t) + C_3(t) \quad (1)$$

Model fits to the PET data were obtained using nonlinear least-squares curve fitting (Bevington, 1969), which utilizes Marquardt's method of minimization (1963).

The model equations that describe the time rate of change of the compartmental concentrations in the brain are

$$\frac{dC_2(t)}{dt} = K_1C_1(t) - (k_2 + k_3)C_2(t) + k_4C_3(t) \quad (2)$$

$$\frac{dC_3(t)}{dt} = k_3C_2(t) - k_4C_3(t) \quad (3)$$

The kinetic parameters K_1 (ml/min/ml) and k_2 (min^{-1}) represent the bidirectional transport of drug across the blood–brain barrier, where K_1 is the plasma clearance. The k_3 (min^{-1}) and k_4 (min^{-1}) parameters reflect the rate constants for binding to and dissociation from receptors,

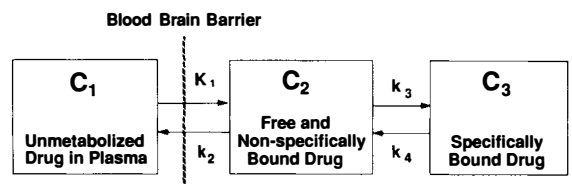

FIG. 1. The three-compartment kinetic model configuration. The kinetic model consists of one vascular compartment (C_1), which contains the unmetabolized drug in plasma, and two extravascular brain compartments, which contain the free and nonspecifically bound drug (C_2) and drug specifically bound to the receptor of interest (C_3). The kinetic analysis provides estimates of the intercompartmental transport parameters, K_1–k_4.

respectively. The first-order dissociation rate constant (k_{off}) is assumed to be equivalent to k_4.

The model equations are linear or nonlinear depending on the degree of receptor occupancy. At high receptor occupancy (low SA), k_3 includes the bound concentration $C_3(t)$:

$$k_3 = k_{on}f_2[B_{max} - C_3(t)] \quad (4)$$

This results in nonlinear model equations as shown in the expanded form of Eq. 3:

$$\frac{dC_3(t)}{dt} = k_{on}f_2B_{max}C_2(t) - k_{on}f_2C_3(t)C_2(t) - k_4C_3(t) \quad (5)$$

where k_{on} (nM^{-1} min^{-1}) is the first-order association rate constant for drug to receptor and f_2 (ml/ml) is the fraction of drug free from nonspecific binding in the brain (Mintun et al., 1984). At low receptor occupancy (high SA), the bound concentration is assumed to be negligible. Equation 4 reduces to

$$k_3 = k_{on}f_2B_{max} \quad (6)$$

and linear model equations result.

The linear and nonlinear pairs of equations were simultaneously fit to the high and low SA data, respectively (Huang et al., 1986, 1989). The four equations were solved using a fourth-order Runge-Kutta numerical integration method with a 0.1-min step. Five kinetic parameters were estimated. The parameters K_1, k_2, k_3 (Eq. 6), and k_4 were assumed to be the same for both sets of data. The fifth parameter $k_{on}f_2$ was determined solely from the low SA data (Sadzot et al., 1991, 1992). The significant C_3 term thus allowed k_3 (Eq. 6) and $k_{on}f_2$ to be estimated as separate kinetic parameters (see Eq. 5).

The binding parameters B_{max} (nM) and K_d (nM) are calculated ratios of the estimated kinetic parameters k_3 (Eq. 6), k_4, and $k_{on}f_2$:

$$B_{max} = \frac{k_3}{k_{on}f_2} = \frac{k_{on}f_2B_{max}}{k_{on}f_2} \quad (7)$$

$$K_d = \frac{k_4}{k_{on}f_2}f_2 = \frac{k_{off}}{k_{on}} \quad (8)$$

The equation for K_d requires that f_2 be known. This parameter was independently calculated for each volunteer using the following relationship (Mintun et al., 1984; Gjedde and Wong, 1990):

$$f_2 = \frac{k_2}{K_1}f_1 \quad (9)$$

An average gray matter K_1/k_2 ratio was obtained from linear three-compartment model fits to nine inhibition study regions. This K_1/k_2 ratio and the subject's average f_1 value (from high and low SA) were used to calculate f_2.

The above equations are consistent for compartmental concentrations expressed in terms of total drug (e.g., nM). However, units of radioactivity concentration (μCi/ml) were used for the simultaneous fits. As implemented, the $k_{on}f_2$ parameter included the low SA (Ci/μmol) and the fifth kinetic parameter was actually $k_{on}f_2$/SA rather than $k_{on}f_2$.

Model configurations. Three model configurations (Methods I–III) were examined. Method I determined the five kinetic parameters simultaneously using no a priori constraints. In Methods II and III, $k_{on}f_2$/SA was fixed to the product of the average value of k_{on} obtained in receptor-rich regions using Method I and each volunteer's mean value of f_2, divided by the volunteer's low SA value. Method II determined four parameters simultaneously. In Method III, the K_1/k_2 ratio was fixed to the inhibition value and only three parameters freely varied. SEs were calculated for B_{max} and K_d using the partial derivatives of the rate constant estimates and the regression covariance matrix (Landaw and DiStefano, 1984). Percentages of (SE/parameter estimate) * 100 were calculated.

RESULTS

Localization of [^{11}C]flumazenil

The regional localization of [^{11}C]flumazenil was consistent with the regional rank order of [^{3}H]flumazenil binding in vitro and with the results obtained by other PET investigators (Persson et al., 1985, 1989*b*; Maloteaux et al., 1988; Pappata et al., 1988; Shinotoh et al., 1989). Images of the radioactivity distribution, at three brain levels, for the volunteer who was scanned three times in a single day are shown in Fig. 2.

In Fig. 2, the three rows of summed images were obtained after the injection of high SA, low SA, and high SA following the administration of 0.15 mg/kg of unlabeled flumazenil, respectively. The first row shows that the distribution of [^{11}C]flumazenil is fairly homogeneous in the cortical areas, lower in the cerebellar and inferior temporal regions, and lowest in the pons region. The middle and bottom rows display the reduction in [^{11}C]flumazenil uptake that occurs as the amount of unlabeled flumazenil increases.

Plasma and blood analyses

Flumazenil metabolism. The Sep-Pak separation of the control samples demonstrated high extraction of the parent drug. The average final extraction determined from the high and low SA results was 95.5 ± 3.1%. The HPLC results demonstrated that no drug metabolism occurred in vitro.

The final Sep-Pak extractions of the postinjection metabolite samples decreased with time. The average final extraction at 5 min was 84.8 ± 5.4% and at 90 min was 76.8 ± 3.2% (high and low SA data pooled). The decreased recovery of total radioactivity was attributed to the increased proportion of the less lipophilic metabolites with time.

The HPLC separation resulted in two peaks that corresponded to unchanged flumazenil (retention time ~7.5 min) and metabolites (retention time ~2.2 min). The relative amounts of the two components for the various time points were used in the determination of the kinetics of metabolized fluma-

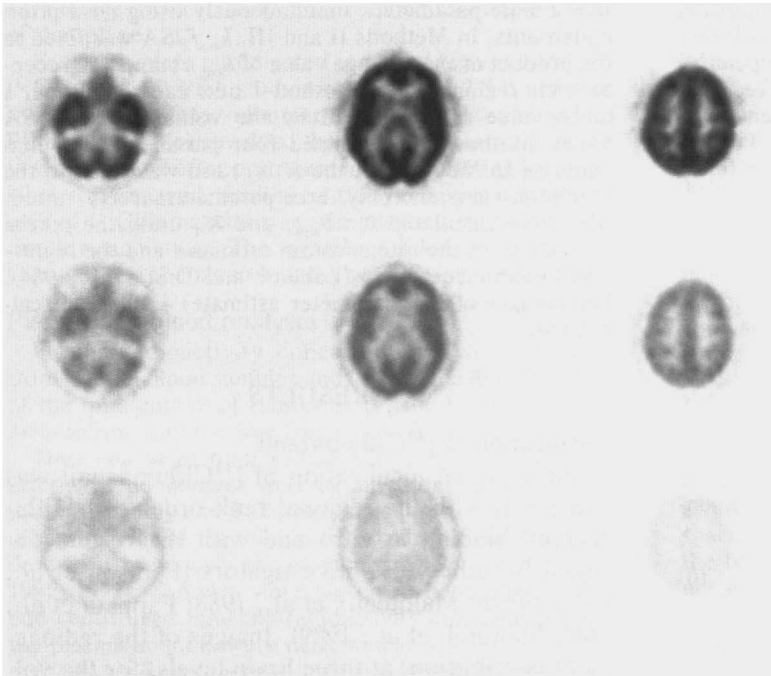

FIG. 2. The summed positron emission tomography images (10–30 min) of the one volunteer who received [^{11}C]flumazenil at high specific activity (SA) **(top),** low SA **(middle),** and high SA **(bottom)** following the injection of 0.15 mg/kg of unlabeled flumazenil. The first row of images display high levels of binding in the neocortical areas, moderate levels in the thalamus, and very low levels in the pons region. The second row of images displays the reduction in uptake that occurred due to the increased occupation of receptors by unlabeled flumazenil. A further reduction in binding is evident in the bottom row of images due to the preinjection of a large dose of unlabeled flumazenil (inhibition study; see text).

zenil in plasma. The HPLC data were corrected for the decreased extraction, discussed above, using the step-by-step extractions of the control and metabolite samples.

The time course of unchanged flumazenil was calculated using linearly interpolated values of the kinetic curve of drug metabolism. The corrected plasma curve was obtained by multiplying the measured total radioactivity by the fraction of unchanged flumazenil. Each subject's measured high and low SA plasma curves were corrected using the unchanged flumazenil data obtained at high and low SA, respectively, for that individual.

The kinetics of radiolabeled metabolites in plasma was fairly rapid for flumazenil. In three of the subjects, the level of metabolized flumazenil was also determined at 2 min. At this early time, an average of ~98% of the radioactivity in plasma corresponded to unchanged flumazenil. However, by 5 min the average value of unchanged flumazenil was ~68% and decreased to ~24% at 90 min. There was no significant difference between the high and low SA kinetics of unchanged flumazenil at 5, 10, 45, and 90 min, with respective p values of 0.16, 0.35, 0.85, and 0.44 (two-sided paired *t* test). However, at 15 min the average low SA fraction of unchanged flumazenil (26.3 ± 2.1) was slightly less than the high SA average (33.7 ± 5.2) ($p = 0.03$, two-sided paired *t* test).

The metabolism results in this work are in agreement with the high SA results reported by Koeppe et al. (1991), Frey et al. (1991), and Debruyne et al. (1991), except for a somewhat greater metabolism in our studies at ~10 min. A curve of the pooled high and low SA results is shown in Fig. 3. The average 2-min value reported above was included in the interpolations for each volunteer as the inclusion of the 2-min plateau improved the fit to the observed PET data at early times.

Free fraction of flumazenil. The average value of f_1 determined for the high SA data was 0.50 ± 0.03 and for the low SA data it was 0.48 ± 0.05. There

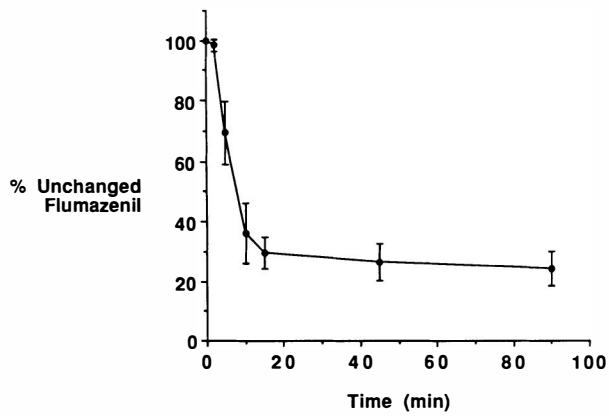

FIG. 3. Time course of unchanged flumazenil in plasma. This curve displays the kinetics of unchanged flumazenil in plasma. The averages were obtained from the pooled high and low specific activity (SA) results for the five volunteers. The 2-min point was measured in only three of the volunteers. There was no significant difference between the high and low SA kinetics of unchanged flumazenil except for the 15-min time point when the average low SA fraction of unchanged flumazenil was slightly less than the high SA average (see text).

was no significant difference between the high and low SA results (p = 0.68, two-sided paired *t* test). Therefore, an average f_1 value was determined for each subject.

There was no significant adsorption of the standard samples to the plastic test tubes. The maximum percentage adsorbed was <2% for the plasma and buffer standards, for the time points examined.

Blood analyses. All of the volunteers had normal electrolyte and blood chemistries. None tested positive for alcohol, acetone, or acetaldehyde.

The radioactivity in the blood samples progressively partitioned in the plasma. At 5 min, the percentage of counts in the red blood cell volume was ~60% of that in whole blood, and by 90 min this percentage had fallen to ~30%. This partitioning suggests that the metabolites of [^{11}C]flumazenil are in the plasma rather than in the red cell fraction.

Kinetic methods

Brain free fraction. An average K_1/k_2 ratio of 0.68 ± 0.08 ml/ml was determined from linear three-compartment model fits to nine gray matter regions of the inhibition study. This K_1/k_2 ratio and the subject's average f_1 value resulted in a mean value of f_2 of 0.72 ± 0.03 ml/ml (Eq. 9).

Method I. Method I required the fewest assumptions but provided some problems with convergence. As expected, the coefficients of variation (CVs) in the estimates and the SEs in B_{max} and K_d were generally larger when five parameters were determined simultaneously. The results obtained using this model configuration are shown in Table 1. The average values of k_3 do not follow the rank order of the B_{max} estimates. The regional k_4 estimates are highly variable, especially in regions with lower receptor concentrations, as are the values of $k_{on}f_2$ and k_{on}.

The average value of k_{on} and its SD increased in regions with lower receptor concentrations where convergence of the model fits was a problem and large CVs (>50%) in the individual kinetic estimates were observed. In fact, the thalamus region could be fit for only one of the volunteers. Method I was used to obtain an estimate of k_{on} by considering only those model fits that were well behaved. Fits to the occipital (n = 5), midtemporal (n = 5), and frontal (n = 4) data were used in this determination, for which the average calculated value of k_{on} was 0.030 ± 0.003 nM^{-1} min^{-1}. The model fits to the frontal data resulted in large CVs in the kinetic estimates for one of the volunteers, and therefore this region was not included in Table 1. The remaining four volunteers yielded average frontal results for K_1, k_2, k_3, k_4, and k_{on} of 0.284 ± 0.048 ml/min/ml, 0.335 ± 0.146 nM^{-1} min^{-1}, 1.25 ± 0.66 nM^{-1} min^{-1}, 0.259 ± 0.109 nM^{-1} min^{-1}, and 0.030 ± 0.011 nM^{-1} min^{-1}, respectively. The B_{max} value was 55.8 ± 25.9 nM and K_d was 8.99 ± 2.95 nM.

Method II. The $k_{on}f_2$/SA constraint applied in Method II removed the convergence difficulties, resulted in adequate fits to thalamus data, and yielded kinetic parameters that were similar to those obtained by Method I. Model fits (Method II) to the

TABLE 1. *Average kinetic parameter estimates obtained using Method I (n = 5)*

	Occipital	Midtemporal	Cerebellum	Inferotemporal	Average	SD	CV (%)
K_1	0.333	0.325	0.303	0.225	0.297	0.049	16.6
SD	0.048	0.035	0.037	0.044			
k_2	0.384	0.437	0.391	0.262	0.369	0.075	20.3
SD	0.216	0.240	0.158	0.131			
k_3	1.62	1.82	2.27	2.75			
SD	0.99	1.48	1.32	2.00			
k_4	0.287	0.277	0.572	0.777	0.478	0.242	50.5
SD	0.073	0.072	0.187	0.560			
$k_{on}f_2$	0.020	0.024	0.049	0.068	0.040	0.023	55.9
SD	0.006	0.011	0.036	0.036			
k_{on}	0.028	0.033	0.069	0.094	0.056	0.031	55.8
SD	0.010	0.015	0.047	0.056			
K_1/k_2	1.06	0.935	0.842	0.964	0.950	0.090	9.5
SD	0.49	0.442	0.237	0.291			
k_3/k_4	5.96	6.38	3.96	4.36			
SD	4.00	3.95	2.21	2.24			
B_{max}	75.7	69.6	52.0	45.7			
SD	31.7	29.8	28.3	23.3			
%SE ± SD	17.4 ± 5.6	16.0 ± 4.7	25.7 ± 7.6	25.2 ± 12.4			
K_d	11.5	9.41	9.75	7.94	9.65	1.46	15.2
SD	5.0	3.96	2.75	2.02			
%SE ± SD	10.1 ± 6.2	11.2 ± 8.7	10.0 ± 4.0	10.1 ± 3.9			

%SE, (standard error/parameter estimate) * 100; CV, coefficient of variation of average parameter estimate; K_1, ml/min/ml; k_2, k_3, and k_4, min^{-1}; k_{on}, nM^{-1} min^{-1} nM^{-1}; B_{max} and K_d, nM.

occipital cortex data of one of the volunteers are shown in Fig. 4. Method II resulted in K_1/k_2 ratios that ranged from 1.07 ± 0.48 in the occipital cortex to 0.61 ± 0.09 in the thalamus. Two of the volunteers had regional K_1/k_2 ratios that were nearly twice as large as in the other volunteers, except in the thalamus region. The B_{max} and K_d estimates are nearly identical to those obtained by Method I while the variability in k_4 is much less (Table 2).

Method III. The regional and intersubject variabilities in the K_1/k_2 ratios were addressed by specifically constraining K_1/k_2 in Method III. The K_1/k_2 ratio was fixed to the average inhibition value to be consistent with the fixed value of $k_{on}f_2/SA$. This method resulted in larger B_{max} estimates especially for the occipital cortex and inferior temporal cortex and a great reduction of the parameter SDs, CVs, and SEs (Table 3). Despite the lower variability, changes in the quality of the fits were visually apparent in only a few cases.

Model comparison, F *test.* The kinetic results were examined by testing whether the additional parameter in Method II resulted in a significantly better fit to the data than Method III, using the F ratio for the additional reduction in sum of squares attributable to the extra parameter. This tested the null hypothesis that Method III is a better model. For the occipital cortex, Method II was the more satisfactory model for the two volunteers with the larger K_1/k_2 ratios ($p < 0.01$), while Method III was better for the remaining volunteers. The cerebellar results showed that Method III was more satisfactory for four of the volunteers, while Method II was for one of the volunteers ($p < 0.01$). For the thalamus, Method III resulted in a significant reduction in the sum of squares for all volunteers, which is consistent with the average K_1/k_2 ratio (0.61 ml/ml) obtained using Method II.

When the F statistic resulted in the rejection of the null hypothesis, Method III yielded binding parameters that were nearly a factor of 2 greater, while the difference was not as great when the null hypothesis was accepted. The percent differences (Method II versus Method III) in the occipital B_{max} estimates were 44.8 and 54.4% for the two volunteers with large K_1/k_2 ratios, while the average difference for the remaining volunteers was <10%. Similarly, the occipital K_d estimates for the two volunteers were 28.5 and 46.9% different, while the average difference for the others was <10%. The regional F test results are consistent with the gradual increase in the k_2 value across the occipital cortex, cerebellum, and thalamus that is evident in the Method II results (Table 2).

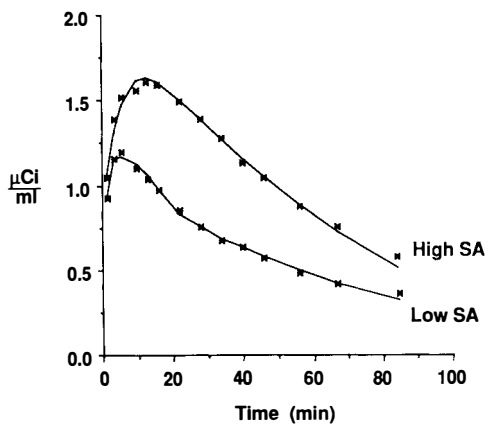

FIG. 4. Simultaneous three-compartment model fits to high and low specific activity (SA) [^{11}C]flumazenil positron emission tomography (PET) data for the occipital cortex. High and low SA [^{11}C]flumazenil PET data were simultaneously fit to linear and nonlinear three-compartment models, respectively. This graph shows examples of typical model fits to the observed occipital PET data.

DISCUSSION

The major finding of this work is that regional measures of BZ receptor B_{max} and K_d can be obtained from simultaneous curve fits of linear and nonlinear three-compartment models to high and low SA [^{11}C]flumazenil PET data, respectively. Various strategies were used in the implementation of the linear and nonlinear models and an optimal method was identified. Nonspecific binding of [^{11}C]flumazenil in brain was not negligible and was accounted for in the models.

Curve-fitting strategy

Sequential and simultaneous curve fittings of the linear and nonlinear models were examined. The first strategy involved sequentially fitting the linear and nonlinear three-compartment models to high and low SA [^{11}C]flumazenil data, respectively. The high SA data were fit with the K_1/k_2 ratio fixed to the high SA pons (reference region) value. Next, the low SA data were fit with the K_1/k_2 ratio fixed to the low SA pons value and k_3 fixed to the k_3 (Eq. 6) value obtained at high SA. This approach resulted in convergence problems and large CVs (>50%) in the individual kinetic parameters. The second strategy was the same as the first except that the low SA pons K_1/k_2 ratio was used for both sets of data. Greater stability in the curve fits, but large CVs in the individual parameters, sometimes resulted when this scheme was used. The third strategy was to simultaneously fit the high and low SA data. Curve fits were performed with the K_1/k_2 ratio fixed to the pons value (four parameters freely varied). However, the same convergence and CV problems

TABLE 2. *Average kinetic parameter estimates obtained using Method II (n = 5)*

	Occipital	Midtemporal	Cerebellum	Inferotemporal	Thalamus	Average	SD	CV (%)
K_1	0.336	0.328	0.332	0.238	0.369	0.321	0.049	15.3
SD	0.058	0.042	0.059	0.038	0.091			
k_2	0.386	0.400	0.444	0.279	0.619	0.426	0.124	29.1
SD	0.221	0.188	0.174	0.123	0.195			
k_3	1.64	1.46	1.20	1.02	0.952			
SD	0.68	0.63	0.53	0.48	0.268			
k_4	0.345	0.292	0.303	0.243	0.239	0.284	0.044	15.5
SD	0.149	0.109	0.070	0.064	0.041			
k_{on} fixed	0.030	0.030	0.030	0.030	0.030			
K_1/k_2	1.07	0.975	0.811	0.939	0.610	0.881	0.177	20.2
SD	0.48	0.419	0.239	0.249	0.085			
k_3/k_4	5.87	5.69	4.11	4.45	4.09			
SD	3.87	3.06	1.98	2.22	1.39			
B_{max}	75.5	67.3	55.6	47.2	44.1			
SD	30.9	27.8	24.2	21.6	12.2			
%SE ± SD	19.1 ± 9.6	16.5 ± 5.9	21.6 ± 5.3	21.1 ± 9.3	26.5 ± 6.4			
K_d	11.5	9.77	10.1	8.13	7.99	9.51	1.47	15.5
SD	5.0	3.67	2.4	2.12	1.36			
%SE ± SD	9.48 ± 5.19	9.09 ± 4.33	9.00 ± 1.95	8.22 ± 1.81	11.1 ± 2.8			

%SE, (standard error/parameter estimate) * 100; CV, coefficient of variation of average parameter estimate; K_1, ml/min/ml; k_2, k_3, and k_4, min^{-1}; k_{on}, nM^{-1} min^{-1}; B_{max} and K_d, nM.

that were encountered with the sequential fits resulted. Finally, simultaneous fits were performed without using pons data. This approach resulted in the lowest CVs in the individual kinetic parameters and SEs in the binding parameter estimates of all strategies examined.

The first sequential method has previously been used successfully to measure human opiate receptor binding parameters from dual SA [^{11}C]diprenorphine PET data (Sadzot et al., 1991, 1992). The lack of success with the sequential fitting of the [^{11}C]flumazenil data is attributed largely to the use of reference region data. The reference region used for the [^{11}C]diprenorphine studies was the occipital cortex, which is more optimally sampled than the pons due to its larger size. Additional measurement errors may arise in the pons data due to the rapid kinetics in that region and spillover radioactivity from adjacent vasculature.

General implementation

There are several general aspects of the quantitative approach that affect the accuracy of the results. First, these studies were performed using a NeuroECAT PET scanner. The direct slice data (32 mm apart) were acquired over two time intervals only in the first 5 min and the final in-plane and axial image resolutions were only ~14.0 mm. Second, the vascular contribution was assumed to be negligible. Five percent of the total plasma concentra-

TABLE 3. *Average kinetic parameter estimates obtained using Method III (n = 5)*

	Occipital	Midtemporal	Cerebellum	Inferotemporal	Thalamus	Average	SD	CV (%)
K_1	0.346	0.338	0.337	0.245	0.359	0.325	0.046	14.0
SD	0.049	0.040	0.057	0.034	0.086			
k_2	0.508	0.496	0.495	0.361	0.528	0.478	0.067	13.9
SD	0.072	0.059	0.084	0.050	0.127			
k_3	2.18	1.84	1.39	1.32	0.820			
SD	0.58	0.39	0.40	0.28	0.115			
k_4	0.285	0.266	0.300	0.230	0.242	0.265	0.029	11.0
SD	0.088	0.075	0.062	0.057	0.041			
k_{on} fixed	0.030	0.030	0.030	0.030	0.030			
K_1/k_2 fixed	0.680	0.680	0.680	0.680	0.680			
k_3/k_4	7.82	7.10	4.68	5.86	3.47			
SD	1.36	0.94	1.06	0.98	0.76			
B_{max}	100	85.0	64.3	60.7	38.0			
SD	25	15.7	17.5	11.5	5.5			
%SE ± SD	3.76 ± 0.71	4.22 ± 0.68	5.57 ± 1.96	4.51 ± 1.10	9.27 ± 2.46			
K_d	9.55	8.91	10.0	7.69	8.11	8.85	0.96	10.9
SD	2.94	2.52	2.1	1.89	1.37			
%SE ± SD	4.43 ± 0.85	4.59 ± 1.19	6.42 ± 2.22	5.33 ± 1.40	10.6 ± 2.6			

%SE, (standard error/parameter estimate) * 100; CV, coefficient of variation of average parameter estimate; K_1, ml/min/ml; k_2, k_3, and k_4, min^{-1}; k_{on}, nM^{-1} min^{-1}; B_{max} and K_d, nM.

tion was subtracted from the total brain concentration to correct for the vascular contribution. However, model fits to these corrected data resulted in convergence problems or kinetic parameters that were unchanged. Third, the model fits were performed using instantaneous model solutions to approximate the observed PET data, which were accumulated over intervals of varying lengths. A small number of integrated model fits were performed. These fits resulted in individual kinetic parameters that were lower in value than those obtained using the instantaneous solutions, but B_{max} and K_d estimates that were very similar (data not shown).

In spite of these limitations and approximations, the K_1 estimates agree with those reported by Koeppe et al. (1991) for the four-parameter model fits to high SA [^{11}C]flumazenil PET data. In addition, the occipital B_{max} and K_d estimates agree with the neocortical estimates obtained from the [^{11}C]flumazenil modeling study performed by Blomqvist et al. (1990) for which there was rapid PET sampling at early times (eight scans of 20 s each).

Assumptions

There are several model-specific assumptions associated with the kinetic methods. First, it was assumed that K_1 is the same for both sets of data. The protein binding studies demonstrated that the free fraction in plasma was the same at high and low SA and the f_1 measurements are consistent with previously reported results (Roncari et al., 1986). These points support the simultaneous determination of K_1 from both sets of data.

Second, the average gray matter K_1/k_2 ratio obtained from the single inhibition study was used to determine f_2 for each volunteer. The K_1/k_2 ratio was estimated from the inhibition data because inaccuracies in the estimate, due to specific binding or partial volume effects, should be minimized using these data. The inhibition K_1/k_2 ratio of 0.68 ± 0.08 ml/ml was similar to the ratios obtained across volunteers in regions where receptor binding was negligible. The averages of the K_1/k_2 ratios for the low SA pons and white matter regions were 0.55 ± 0.19 and 0.68 ± 0.17 ml/ml, respectively. These points support the validity of using the average regional inhibition K_1/k_2 ratio to determine f_2 for each volunteer.

The third assumption concerns the k_{on} value used in the $k_{on}f_2$/SA constraint of Methods II and III. The average k_{on} estimate obtained for receptor-rich regions was applied to all regions. The greater reliability of the receptor-rich k_{on} estimate is thought to reflect its better estimation in regions with higher receptor binding. In going from Method I to Method II, there were no convergence difficulties, the variability in the regional k_4 estimates was reduced, adequate fits were obtained for all regions, the k_3 estimates followed the rank order of regional binding, and the parameter estimates were in close agreement between the methods. The binding parameters were fairly insensitive to changes in the $k_{on}f_2$/SA constraint as is especially evident when comparing the inferior temporal cortex results obtained by Methods I and II. The last point is consistent with the finding of Huang et al. (1989) that a 10% error in a similar constraint, k_d/f_2k_a, resulted in a change of <3% in the B_{max} estimate.

Fourth, a regionally homogeneous free fraction was assumed when using the fixed value of $k_{on}f_2$/SA in Methods II and III. The variability of the inhibition K_1/k_2 ratio was ~11%, which supports the use of one value of f_2 for all regions. Other factors related to this assumption are included in the comparison below.

Comparison of simultaneous methods

The simultaneous F ratios (null hypothesis: Method III is a better model) indicated that the occipital data of two volunteers and the cerebellar data of one volunteer were not significantly better fit when the K_1/k_2 ratio was specifically constrained to 0.68 ml/ml (Method III). For all volunteers, Method III was a more satisfactory method for the thalamic data, although this was expected because the average K_1/k_2 ratio determined by Method II was 0.61 ml/ml. The rejection of the null hypothesis resulted in binding parameters that were nearly a factor of 2 different between the two methods, while acceptance of the hypothesis resulted in a much smaller difference. The source of this difference was not determined. In view of these points, Method II proved to be a satisfactory method for each volunteer across all regions, while Method III was a better method for three of the five volunteers.

Methods II and III rely on a regionally uniform value of f_2. The average K_1/k_2 ratios determined by Method II varied across regions (Table 2), which is inconsistent with a fixed value of f_2. The cortical ratios were larger than those for regions with lower receptor concentrations. When regional values of f_2 were calculated using the average K_1/k_2 ratios in Table 2, the mean regional K_d value decreased to 8.1 ± 1.2 nM (−15% difference). The difference was greatest for the occipital cortex for which the K_d estimate went from 11.5 nM (inhibition f_2 = 0.72) to 8.52 nM (occipital f_2 = 0.54).

A possible explanation for both the regional variability in the Method II K_1/k_2 ratios and the com-

paratively larger Method III B_{max} estimates can be found in the results of the cyclofoxy rat studies performed by Kawai et al. (1991). Opiate receptor binding parameters were estimated using an equilibrium (bolus + constant infusion) protocol. In these studies, errors resulted from the use of reference region (cerebellum) nonspecific binding for all brain regions. Overestimations of B_{max} and K_d for cortical regions were as large as sixfold and about twofold for the thalamus. The binding parameters were fairly well estimated for regions with nonspecific binding that was comparable with that in the cerebellum. This explanation might support the use of Method II over Method III. However, the applicability of the findings from equilibrium cyclofoxy rat studies to human [^{11}C]flumazenil PET studies is uncertain. Furthermore, nonspecific binding may not be as great a factor for flumazenil as for cyclofoxy. This is plausible because nonspecific binding was found to be negligible in tracer [^{3}H]flumazenil animal studies (Goeders and Kuhar, 1985), the in vivo measure of f_2 (0.72) is large, and the regional variability in the inhibition K_1/k_2 ratios is low.

Method II was satisfactory for each volunteer across regions, but the physiological interpretation of a regionally variable f_2 is unclear, particularly since the inhibition study resulted in a fairly uniform value of f_2. In comparison, Method III was more often a better method, is physiologically consistent with a uniform value of f_2, and resulted in considerably lower parameter variability than Method II. The reduction in variability may be at the expense of adding bias to the parameters, but is an important factor given the small number of subjects studied. Method III is the best simultaneous method overall due to its physiological consistency and low parameter variability.

Relation to previous models

There are a few general issues of neuroreceptor binding studies that are important to address with respect to this and previous work. One critical issue for neuroreceptor studies is the effect of receptor occupancy on the estimation of the binding parameters. As stated by Kawai et al. (1991), large experimental errors result in regions with high receptor concentrations when the difference between nonspecifically bound and receptor-bound tracer is small (plasma concentration of drug is too high). Similarly, if the concentration of drug is too low, insufficient receptor occupancy results. In this work, receptor occupancies and volumes of distribution were determined using the parameters obtained by Method II. The maximal receptor occupancy achieved at high SA was $<1\%$ and at low SA $\sim 75\%$ when averaged across the five volunteers. The volumes of distribution of free, nonspecifically bound, and receptor-bound drug were determined using λ_w, f_1, K_1, k_2, k_3, and k_4 in the relationships described by Sawada et al. (1990) and Koeppe et al. (1991). In the occipital cortex, the volumes of distribution of free and nonspecifically bound drug were, respectively, ~ 6.5 and 10.3% of the receptor-bound volume of distribution. In the cerebellum, the corresponding percentages were 12.4 and 13.0%. Accordingly, the receptor occupancies used in this work are in a range that permits accurate parameter estimation. Future studies will evaluate the effect of the high and low SA receptor occupancies on the errors in the parameter estimates.

Another issue is the use of equilibrium and negligible nonspecific binding assumptions in previous analyses of [^{11}C]flumazenil PET studies. These assumptions were not valid for the data in this work as demonstrated by two basic results. First, true equilibrium was not established following the bolus injection of the high or low SA [^{11}C]flumazenil. Second, the kinetic results yielded an average f_2 value of 0.72, which is inconsistent with an assumption of negligible nonspecific binding.

A third point concerns the use of simplified models to obtain measures of receptor binding. The kinetic analyses of high SA [^{11}C]flumazenil data performed by Koeppe et al. (1991) utilized a two-compartment model to estimate total ligand distribution volumes. This is a valuable approach because the distribution volumes reflect specific binding while requiring the estimation of only two parameters from the data. In the present work, steady state was most consistently demonstrated at high SA as demonstrated by Patlak plots (Patlak and Blasberg, 1985). However, a two-compartment model was inadequate for the low SA data. Graphical analyses of the low SA data demonstrated that steady state did not always occur and, if so, was short-lived at variable times near the middle of the study (data not shown). The two-compartment model underestimated the low SA radioactivity concentration after 25 min by $\sim 30\%$ and two exponentials were required. This is consistent with the finding of Koeppe et al. (1991) that the best two-compartment model fits were obtained in regions with high receptor concentrations. The additional exponential term may be needed to account for large variations in receptor occupancy due to the increased clearance of bound radioactivity by unlabeled drug.

Finally, the use of the pons as a reference region resulted in problems for all kinetic methods, and the inhibition data proved best for this work. Sawada et

al. (1990) have described the determination of the free brain concentration and the K_1/k_2 ratio using the free fraction in plasma and the tissue/plasma water partition coefficient. This approach is another example of how distribution volumes can be used effectively in place of individual parameter estimates. This method is particularly suited for equilibrium analyses because nonspecific binding in brain is not a complicating factor. The kinetic method, however, requires information about nonspecific binding and the estimation of f_2 would still require curve fitting.

In conclusion, kinetic modeling was used to obtain regional BZ receptor binding parameters from dual SA [^{11}C]flumazenil PET data. This study demonstrated that non-steady-state kinetic methods can be used to determine binding parameters for PET radiotracers with ample blood–brain barrier extraction and rapidly reversible binding.

Acknowledgment: This work was supported by USPHS grants AG 08740 and NS 15080. The authors are grateful to Henry N. Wagner, Jr., MD., for creating a productive working environment and for sponsoring our development as independent scientific investigators. We appreciate the helpful comments of Drs. Richard E. Carson and Kenneth H. Douglass and influential thoughts of Dr. Niels A. Lassen. The authors also thank John Flesher, B.A., Hans Mueller-Gaertner, M.D., Christina Cromwell, B.A., Madge Murrell, R.N., David Clough, C.N.M.T., Emma Rivera-Luna, C.N.M.T., William Boitnott, C.N.M.T., T. K. Natarajan, Sc.D., Darrell Burckhardt, B.A., Helen Drew, C.N.M.T., Joanna Schmidt, C.N.M.T., and Robert C. Smoot, C.N.M.T., for their assistance in the performance of the experiments.

REFERENCES

Abadie P, Baron JC, Bisserbe JC, Boulenger JP, Rioux P, Travère JM, Barre L, Petit-Taboue MC, Zarifian E (1992) Central benzodiazepine receptors in human brain: estimation of regional B_{max} and K_D values with positron emission tomography. *Eur J Pharmacol* 213:107–115

Altman PL (1961) Analysis and compilation. In: *Biological Handbooks: Blood and Other Body Fluids* (Dittman DS, ed), Washington, DC, FASEB, p 19

Bevington PR (1969) *Data Reduction and Error Analysis for the Physical Sciences*. New York, McGraw-Hill, pp 204–246

Blomqvist G, Pauli S, Farde L, Eriksson L, Persson A, Halldin C (1990) Maps of receptor binding parameters in the human brain—a kinetic analysis of PET measurements. *Eur J Nucl Med* 16:257–265

Comar D, Mazière M, Godot JM, Berger G, Soussaline F, Menini C, Arfel G, Naquet R (1979) Visualisation of ^{11}C-flunitrazepam displacement in the brain of the live baboon. *Nature* 280:329–331

Comar D, Mazière M, Cepeda C, Godot JM, Menini C, Naquet R (1981) The kinetics and displacement of [^{11}C]flunitrazepam in the brain of the living baboon. *Eur J Pharmacol* 75:21–26

Dannals RF, Ravert HT, Wilson AA, Wagner HN Jr (1986) An improved synthesis of (3-*N*-[^{11}C]methyl)spiperone. *Appl Radiat Isot Int J Appl Instrum* [*A*] 37:433–434

Dannals RF, Ravert HT, Wilson AA, Wagner HN Jr (1990) Synthesis of a selective serotonin uptake inhibitor: [^{11}C]citalopram. *Appl Radiat Isot Int J Radiat Appl Instrum* [*A*] 41: 541–543

Darragh A, Lambe R, O'Boyle C, Kenny M, Brick I (1983) Absence of central effects in man of the benzodiazepine antagonist RO 15-1788. *Psychopharmacology* 80:192–195

Debruyne D, Abadie P, Barre L, Albessard F, Moulin M, Zarifian E, Baron JC (1991) Plasma pharmacokinetics and metabolism of the benzodiazepine antagonist [^{11}C] Ro 15-1788 (flumazenil) in baboon and human during positron emission tomography studies. *Eur J Drug Metab Pharmacol* 16:141–152

de la Sayette V, Chavoix C, Brouillet E, Hantraye P, Kunimoto M, Khalili-Varasteh M, Guibert B, Prenant C, Mazière M (1991) In vivo benzodiazepine receptor occupancy by CL 218,872 visualized by positron emission tomography in the brain of the living baboon: relation with anticonvulsant activity. *Exp Brain Res* 83:397–402

Frey KA, Holthoff VA, Koeppe RA, Jewett DM, Kilbourn MR, Kuhl DE (1991) Parametric in vivo imaging of benzodiazepine receptor distribution in human brain. *Ann Neurol* 30: 663–672

Frost JJ, Wagner HN Jr, Dannals RF, Ravert HT, Wilson AA, Links JM, Rosenbaum AE, Trifiletti R, Snyder SH (1986) Imaging benzodiazepine receptors in man with ^{11}C-suriclone by positron emission tomography. *Eur J Pharmacol* 122: 381–383

Frost JJ, Douglass KH, Mayberg HS, Dannals RF, Links JM, Wilson AA, Ravert HT, Crozier WC, Wagner HN Jr (1989) Multicompartmental analysis of [^{11}C]carfentanil binding to opiate receptors in man measured by positron emission tomography. *J Cereb Blood Flow Metab* 9:398–409

Gjedde A, Wong DF (1990) Modeling neuroreceptor binding of radioligands in vivo. In: *Quantitative Imaging: Neuroreceptors, Neurotransmitters, and Enzymes* (Frost JJ, Wagner HN Jr, eds), New York, Raven Press, pp 51–79

Goeders NE, Kuhar MJ (1985) Benzodiazepine receptor binding *in vivo* with [^{3}H]-Ro 15-1788. *Life Sci* 37:345–355

Hantraye P, Kaijima M, Prenant C, Guibert B, Sastre J, Crouzel M, Naquet R, Comar D, Mazière M (1984) Central type benzodiazepine binding sites: a positron emission tomography study in baboon's brain. *Neurosci Lett* 49:115–120

Hantraye P, Brouillet E, Fukuda H, Chavoix C, Guibert B, Dodd R, Prenant C, Crouzel M, Naquet R, Mazière M (1988) Benzodiazepine receptors studied in living primates by positron emission tomography: antagonist interactions. *Eur J Pharmacol* 153:25–32

Hoffman EJ, Phelps ME, Huang SC (1983) Performance evaluation of a positron tomograph designed for brain imaging. *J Nucl Med* 24:245–257

Holthoff VA, Koeppe RA, Frey KA, Paradise AH, Kuhl DE (1991) Differentiation of radioligand delivery and binding in the brain: validation of a two-compartment model for [^{11}C]flumazenil. *J Cereb Blood Flow Metab* 11:745–752

Huang S-C, Barrio JR, Phelps ME (1986) Neuroreceptor assay with positron emission tomography: equilibrium versus dynamic approaches. *J Cereb Blood Flow Metab* 6:515–521

Huang S-C, Bahn MM, Barrio JR, Hoffman JM, Satyamurthy N, Hawkins RA, Mazziotta JC, Phelps ME (1989) A double injection technique for in vivo measurement dopamine D2-receptor density in monkeys with 3-(2′-[^{18}F]fluoroethyl)spiperone and dynamic positron emission tomography. *J Cereb Blood Flow Metab* 9:850–858

Iyo M, Itoh T, Yamasaki T, Fukuda H, Inoue O, Shinotoh H, Suzuki K, Fukui S, Tateno Y (1991) Quantitative in vivo analysis of benzodiazepine binding sites in the human brain using positron emission tomography. *Neuropharmacology* 30:207–215

Kawai R, Carson RE, Dunn B, Newman AH, Rice KC, Blasberg RG (1991) Regional brain measurement of B_{max} and K_D with the opiate antagonist cyclofoxy: equilibrium studies in the conscious rat. *J Cereb Blood Flow Metab* 11:529–544

Koeppe RA, Holthoff VA, Frey KA, Kilbourn MR, Kuhl DE

(1991) Compartmental analysis of [^{11}C]flumazenil kinetics for the estimation of ligand transport rate and receptor distribution using positron emission tomography. *J Cereb Blood Flow Metab* 11:735–744

Landaw EM, DiStefano JJ III (1984) Multiexponential, multicompartmental, and noncompartmental modeling. II. Data analysis and statistical considerations. *Am J Physiol* 246:R665–R677

Maloteaux JM, Octave JN, Vanisberg MA, Kollmann P, Ackermans A, Laterre C (1988) Benzodiazepine receptors in human brain: characterization, subcellular localization and solubilization. *Prog Neuropsychopharmacol Biol Psychiatry* 12:773–782

Marquardt DW (1963) An algorithm for least squares estimation of nonlinear parameters. *J Soc Ind Appl Math* 2:431–441

Mazière M, Prenant C, Sastre J, Crouzel M, Comar D, Hantraye P, Kajjima M, Guibert B, Naquet R (1983) ^{11}C-RO 15 1788 et ^{11}C-flunitrazepam, deux coordinats pour l'etude par tomographie par positons des sites de liaison des benzodiazepines. *CR Acad Sci (Paris)* 296:871–876

Mintun MA, Raichle ME, Kilbourn MR, Wooten GF, Welch MJ (1984) A quantitative model for the in vivo assessment of drug binding sites with positron emission tomography. *Ann Neurol* 15:217–227

Pappata S, Samson Y, Chavoix C, Prenant C, Mazière M, Baron JC (1988) Regional specific binding of [^{11}C]Ro 15-1788 to central type benzodiazepine receptors in human brain: quantitative evaluation by PET. *J Cereb Blood Flow Metab* 8: 304–313

Patlak CS, Blasberg RG (1985) Graphical evaluation of blood-to-brain transfer constants from multiple-time uptake data. Generalizations. *J Cereb Blood Flow Metab* 5:584–590

Perlmutter JS, Kilbourn MR, Welch MJ, Raichle ME (1989) Non-steady-state measurement of in vivo receptor binding with positron emission tomography: "dose-response" analysis. *J Neurosci* 9:2344–2352

Persson A, Ehrin E, Eriksson L, Farde L, Hedstrom CG, Litton JE, Mindus P, Sedvall G (1985) Imaging of [^{11}C]-labelled Ro 15-1788 binding to benzodiazepine receptors in the human brain by positron emission tomography. *J Psychiatr Res* 19: 609–622

Persson A, Pauli S, Swahn CG, Halldin C, Sedvall G (1989*a*) Cerebral uptake of ^{11}C-Ro 15-1788 and its acid metabolite ^{11}C-Ro 15-3890; PET study in healthy volunteers. *Hum Psychopharmacol* 4:215–220

Persson A, Pauli S, Halldin C, Stone-Elander S, Farde L, Sjogren I, Sedvall G (1989*b*) Saturation analysis of specific ^{11}C Ro 15-1788 binding to the human neocortex using positron emission tomography. *J Neurosci Methods* 4:21–31

Roncari G, Ziegler WH, Guentert TW (1986) Pharmacokinetics of the new benzodiazepine antagonist Ro 15-1788 in man following intravenous and oral administration. *Br J Clin Pharmacol* 22:421–428

Sadzot B, Price JC, Mayberg HS, Douglass KH, Dannals BF, Lever JR, Ravert HT, Wilson AA, Wagner HN Jr, Feldman MA, Frost JJ (1991) Quantification of human opiate receptor concentration and affinity using high and low specific activity [^{11}C]diprenorphine and positron emission tomography. *J Cereb Blood Flow Metab* 11:204–219

Sadzot B, Price JC, Mayberg HS, Douglass KH, Dannals BF, Lever JR, Ravert HT, Wilson AA, Wagner HN Jr, Feldman MA, Frost JJ (1992) Erratum: quantification of human opiate receptor concentration and affinity using high and low specific activity [^{11}C]diprenorphine and positron emission tomography. *J Cereb Blood Flow Metab* 12:885

Samson Y, Hantraye P, Baron JC, Soussaline F, Comar D, Mazière M (1985) Kinetics and displacement of [^{11}C]Ro 15-1788, a benzodiazepine antagonist, studied in human brain in vivo by positron tomography. *Eur J Pharmacol* 110:247–251

Savic I, Persson A, Roland P, Pauli S, Sedvall G, Widen L (1988) In vivo demonstration of reduced benzodiazepine receptor binding in human epileptic foci. *Lancet* 2:863–866

Sawada Y, Hiraga S, Francis B, Patlak C, Pettigrew K, Ito K, Owens E, Gibson R, Reba R, Eckelman W, Larson S, Blasberg RG (1990) Kinetic analysis of 3-quinuclidinyl 4-[^{125}I]iodobenzilate transport and specific binding to muscarinic acetylcholine receptor in rat brain in vivo: implications for human studies. *J Cereb Blood Flow Metab* 10:781–807

Shinotoh H, Yamasaki T, Inoue O, Itoh T, Suzuki K, Hashimoto K, Tateno Y, Ikehira M (1986) Visualization of specific binding sites of benzodiazepine in human brain. *J Nucl Med* 27:1593–1599

Shinotoh H, Iyo M, Yamada T, Inoue O, Suzuki K, Itoh T, Fukuda H, Yamasaki T, Tateno Y, Hirayama K (1989) Detection of benzodiazepine receptor occupancy in the human brain by positron emission tomography. *Psychopharmacology* 99:202–207